Long-term performance and life cycle assessment of energy piles in three different climatic conditions

Melis Sutman [a, *], Gianluca Speranza [a, b], Alessio Ferrari [a], Pyrène Larrey-Lassalle [b], Lyesse Laloui [a]

[a] *Swiss Federal Institute of Technology in Lausanne, EPFL, Laboratory of Soil Mechanics, LMS, Station 18, CH 1015, Lausanne, Switzerland*
[b] *Nobatek/INEF4, 67 Rue de Mirambeau, F-64600, Anglet, France*

ARTICLE INFO

ABSTRACT

The main purpose behind the use of energy piles is to enable the exploitation of geothermal energy for meeting the heating/cooling demands of buildings in an efficient and environment-friendly manner. However, the long-term performance of energy piles in different climatic conditions, along with their actual environmental impacts, has not been fully assessed. In this paper, the results of a finite element model taking into consideration the heating and cooling demands of a reference building, and the intermittent operation of a ground source heat pump, are revealed to examine the long-term performance of energy piles. Furthermore, a life cycle assessment model is implemented to compare the environmental performance of energy piles and a group of conventional piles. The environmental enhancement provided by the adoption of a ground source heat pump system is quantified with respect to a conventional heating and cooling system. The obtained results show that (i) the energy pile system can meet the majority of the heating/cooling demands, except during the peak demands, (ii) the geothermal operation results in temperature fluctuations within the energy piles and the soil, (iii) the use of energy piles results in a significant reduction in environmental impacts in the majority of the examined cases.

© 2019 The Authors. Published by Elsevier Ltd. This is an open access article under the CC BY license (http://creativecommons.org/licenses/by/4.0/).

1. Introduction

Global energy requirements are expected to expand by 30% by 2040 as a result of global economy growth with an annual rate of 3.4%, a projected population increase of 1.6 billion, and inevitably increasing urbanisation [1]. Space heating and cooling is the world's largest energy sector, for instance, it accounts for 50% of the final energy consumption of Europe [2]. It was also responsible for 28% of global energy-related CO_2 emissions in 2017 [3]. Fossil-fuel-based and conventional electric equipment still dominate the global building market, which accounts for more than 80% of the heating equipment [4]. Moreover, owing to global warming, economic growth, and urbanisation, the use of energy for space cooling has more than tripled between 1990 and 2016 [5]. In this context, the development and diffusion of reliable, economically viable, and environment-friendly technologies for meeting a significant

portion of the energy requirements of the building sector is an important challenge.

The energy pile concept is a technology that enables the use of renewable energy sources for efficient space heating and cooling. In this system, the piles that are already required for structural support are equipped with geothermal loops for performing heat exchange operations to exploit the near-surface geothermal energy. The idea behind the energy geostructures comes from the fact that the temperature of the ground remains the same throughout the year after a certain depth (8–10 m). Therefore, with the integration of the geothermal loops and the heat carrier fluid circulating within them, the heat is extracted from the ground to heat the buildings during winter. Similarly, during summer, the extra heat is injected into the ground to cool them. In this system, ground source heat pumps (GSHP) are often required which work intermittently in order to adapt the temperature of the circulating fluid to meet the energy demands from the building side.

Given the great potential of energy piles for reducing the dependency on fossil fuels, various in situ tests were performed on this subject [6–12]. Moreover, several models or tools with varying

---

* Corresponding author.
 E-mail address: melis.sutman@epfl.ch (M. Sutman).

complexity were developed for the analysis and design of energy piles [13–18]. Although the previous research has answered the majority of the fundamental questions on the mechanisms governing the thermo-mechanical behaviour of energy piles, in these studies the temperature changes have been imposed to the test piles instead of being natural consequences of an actual operation. In a few studies, the long-term behaviour of energy piles employed in real operations have been monitored [19–21]. Nevertheless, no experimental data has yet been published in order to perform a systematic comparison of the long-term performance of energy piles under different climatic conditions, i.e., energy piles being subjected to various heating and cooling demands. In addition, although the role of geotechnical engineering in sustainable development is being increasingly recognized [22], there still exist uncertainties related to the actual environmental impact of these so-called green geostructures on their life cycle (LC), which is influenced by the material production, transportation, execution, use, and end of life (EOL) and greatly depends on the demand/supply relationship between the upper structure and energy piles.

Considering the above-mentioned challenges, a 3D finite element model for a group of energy piles was developed which is capable of taking into consideration the real operating philosophy of a GSHP, i.e., intermittent operation. Moreover, the actual space heating and cooling demands of a reference office building from three cities in Europe (Seville, Spain; Rome, Italy; and Berlin, Germany) were employed in the model to represent three diverse climatic conditions (warm, mild, and cold, respectively). In this paper, the numerical model is first described in detail. The heating and cooling demands versus supply data, temperature of the heat carrier fluid as well as of the piles and the soil are then reported for the purpose of comparison. Next, a life cycle assessment (LCA) model is implemented to estimate the environmental impacts of the energy piles employed in the different cities. Finally, a comparison with a conventional heating and cooling system is presented in terms of human health, ecosystem quality, climate change, and resource depletion.

2. Material and methods

One of the main goals of this study is the assessment of the long-term performance of energy piles in different climatic conditions (i.e., different heating and cooling demands). To obtain a thorough comparison in this respect, the space heating and cooling demands for a reference building type at different climatic conditions should be employed as the input in numerical simulations. The ENTRANZE Project [23,24] presents the necessary data for this purpose, where the heating and cooling energy demands for four different reference building types (single family house, apartment block, office building, and school) are systematically determined using the whole building energy simulation program, EnergyPlus. Among the reference buildings employed in the ENTRANZE Project, the reference office building was selected for the analysis presented in this paper. The reference building is a medium-size, five-story building with 3-m high floors. The net heated area of the building is 2400 m^2. Each floor of the building is of the same size of 30 m × 16 m, in length and width, respectively.

Within the ENTRANZE Project, 10 key cities, in other words ten climatic conditions, in Europe are reported to be selected for building energy simulations while considering the winter severity index (WSI), summer severity index (SSI), and climatic cooling potential (CCP) as indicators. From among the 10 cities, three were selected for the present study: Seville, Rome, and Berlin. These cities, in particular, were selected to represent three different climatic conditions and diverse space heating and cooling demands (Fig. 1). Seville, with a high SSI and low WSI, represents the case of a

heat pump operation more on the cooling side. In contrast, Berlin represents a case with high heating and significantly low cooling demands. Furthermore, the heating–cooling demands in Rome lie between those of the two former cities with almost balanced space heating and cooling requirements.

2.1. 3D finite element modelling of an energy pile group

A 3D time-dependent finite element model (Fig. 2a) was built using the COMSOL Multiphysics Software [25] to investigate the long-term performance of energy piles, thus allowing the intermittent operation of the heat pump. In other words, in the presented model, the heat pump operates until the daily heating/cooling demand of the building is met, following which the operation is automatically terminated until the next day. The intermittent operation of the heat pump allows the temperatures of the pile and soil to recover to some extent during the stoppage times, which is also the case for the actual geothermal operations of energy piles. The heating–cooling demands presented in the previous section were employed in the model for this purpose. Although the employed mathematical formulation has proved to be adequate in modelling heat transfer in pipes and porous media regarding energy piles [11], the enhancement of the model with GSHP remains to be corroborated with the experimental data becoming available.

With reference to the foundation of the reference building, 32 piles that were 0.5 m in diameter and 20 m in length were employed. The piles had a 4.75-m and 5.25-m centre-to-centre spacing in the x- and y-directions, corresponding to pile spacing ratios of 9.5 and 10.5, respectively (Fig. 2b). Each pile was equipped with a single U-loop pipe, with a central distance of 0.3 m between the entering and exiting pipes.

Regarding the discretization of the model, mesh independence analyses were performed and element quality was controlled systematically in order to avoid erroneous interpretation of the model results. The model comprises of extremely fine and extra fine meshes of 902,104 elements in total to characterize the soil (590,509 elements) and pile (311,595 elements) domains. Tetrahedral, triangular, linear and vertex elements were employed to describe the finite element model. Regarding the pipes, Pipe Flow Module of COMSOL Multiphysics Software was employed, which idealizes the 3D flow within pipes to edge elements. The mesh for the pipes were defined by 8075 edge elements.

2.1.1. Mathematical formulation

In the presented model, the heat transfer in the porous media module was employed for the pile and soil domains [25]. The soil domain was assumed to be isotropic and fully saturated with water. For both the soil and pile domains, equivalent thermal properties characterising the fluid and solid phases were assigned, and pure thermal conductivity was anticipated, which is governed by the following equation:

$$\rho c \frac{\partial T}{\partial t} - \text{div}(\lambda \mathbf{grad} T) = 0 \tag{1}$$

where ρ is the density, c and λ are the specific heat capacity and thermal conductivity, respectively, including both fluid and solid components, T is the temperature, and div and **grad** are the divergence and gradient operators, respectively. With respect to the heat transfer in the pipes within the energy piles, the following equation was employed while considering an incompressible fluid in the pipes:
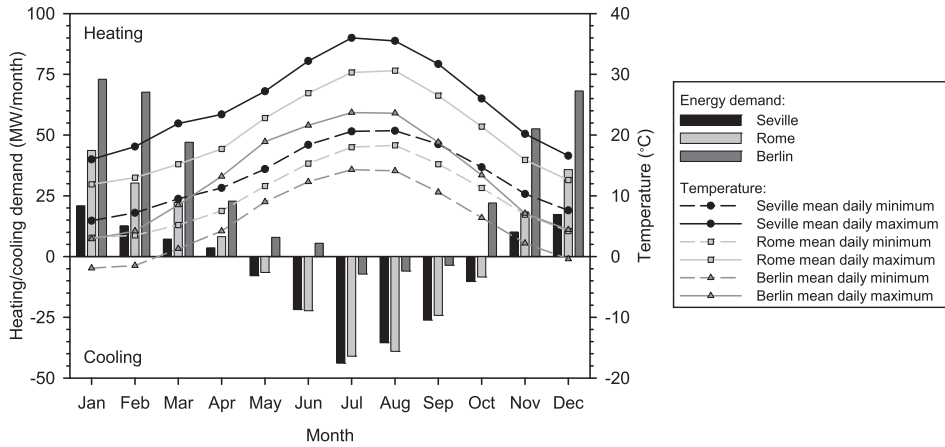
Fig. 1. Heating/cooling demand histogram; minimum and maximum mean daily temperatures at Seville, Rome, and Berlin.
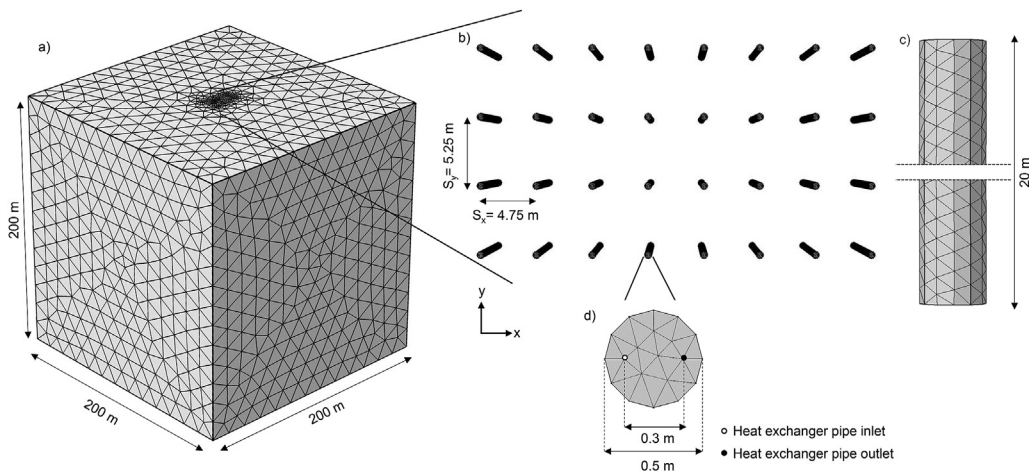

Fig. 2. a) Finite element mesh; b) Energy pile foundation layout; c) Energy pile geometry and pipe positions.

$$\rho_f A_p c_f \frac{\partial T_f}{\partial t} + \rho_f A_p c_f \boldsymbol{u_{f,i}} \cdot \mathbf{grad} T_f = \mathrm{div}\left(A_p \lambda_f \mathbf{grad} T_f\right) + \frac{1}{2} f_D \frac{\rho_f A_p}{d_h} |\boldsymbol{u}|^3 + q'_w$$

(2)

where ρ_f, c_f, and λ_f are the density, specific heat capacity, and thermal conductivity of the fluid, respectively; A_p and d_h are the cross-sectional area and hydraulic diameter of the pipe, respectively; T_f is the temperature of the fluid; $u_{f,i}$ is the velocity vector; and f_D is the Darcy friction factor. q'$_w$ represents the heat transfer through the unit length of the pipe wall and is governed by the following equation:

$$q'_w = 2h_{eff}\pi r_{in}\left(T_{out} - T_f\right)$$

(3)

where r_{in} and T_{out} are the inner diameter and outer temperature of the pipe, respectively, and h_{eff} is the effective heat transfer coefficient of the pipe, which is governed by the following equation:

$$h_{eff} = \frac{2\pi}{\frac{1}{r_{in}h_{int}} + \frac{\ln\left(r_{out}/r_{in}\right)}{\lambda_p}}$$

(4)

where r_{out} and λ_p are the outer diameter and thermal conductivity of the pipe, respectively, and h_{int} is the convective heat transfer coefficient inside the pipe, which is obtained using the following equation:

$$h_{int} = Nu\frac{\lambda_f}{d_h}$$

(5)

The Nusselt number (Nu) is the ratio of the convective to conductive heat transfer across a boundary and is given by the below equation:

$$Nu_{turb} = \frac{\left(f_D/8\right)(Re - 1000)Pr}{1 + 12.7\sqrt{f_D/8}\left(Pr^{\frac{2}{3}} - 1\right)}$$

(6)

The Reynolds number (Re) is the ratio of the inertial forces to viscous forces (Equation (7)), and the Prandtl number (Pr) is the ratio of the momentum diffusivity to thermal diffusivity (Equation (8)).

$$Re = \frac{\rho_f u d_h}{\mu_f}$$

(7)

$$Pr = \frac{\mu_f c_f}{\lambda_f} \tag{8}$$

Finally, the Darcy friction angle can be obtained using a simplified Haaland Equation [26] for a low relative roughness, Colebrook Equation [27], as shown below:

$$\sqrt{\frac{1}{f_D}} = -1.8 log_{10} \left(\frac{6.9}{Re} \right) \tag{9}$$

2.1.2. Boundary and initial conditions

The Neumann boundary condition with no heat flux is assigned to the ground surface since in most energy pile applications, thermal insulation is ensured between the slab and the upper environment. On the other hand, prescribed temperature (Dirichlet) boundary condition is specified for the vertical sides and the bottom boundary. The size of the soil domain is taken large enough at distances where the heat exchange operations have no effect, in order to avoid any boundary effects. The average annual ground temperatures for three cities, which is determined by relating the air temperature to the ground temperature [28], are assigned to the vertical sides and bottom boundaries, as well as to all the materials used in the model as the initial condition.

2.1.3. Material properties

In the presented model, the climatic conditions of the three cities were used to define the average ground temperature and also the heating and cooling demands from the building side. However, the soil conditions and material properties were the same for the three cities for the purpose of systematically comparing the long-term response of energy piles to three different energy demands. The soil domain in the model is assumed to be isotropic, fully saturated, medium dense sand. The pile domain is assumed to be reinforced concrete. The material properties for both the soil and pile domains are presented in Table 1. Table 2 presents the properties assigned to the pipes for which 1-inch, cross-linked poly-ethylene (PEX) pipe type was assumed. Regarding the water circulating within the pipes, temperature-dependent properties were assigned for the density, thermal conductivity and specific heat capacity determined by Ref. [29].

2.1.4. Idealised heat pump

A 30-kW water-to-water heat pump is used in the analysis conducted for the three reference cities. To simulate the intermittent operation of the heat pump, indicator states are included in the model, which monitor whether the daily heating/cooling demand is fulfilled for each time step. Once the demand is fulfilled, the heat pump operation stops until the next day, but the water still continues to flow within the pipes, thus allowing thermal recovery.

A schematic of the GSHP system is presented in Fig. 3 to demonstrate the three main sections: primary circuit (between the ground and GSHP), GSHP and secondary circuit (between the GSHP and building), as well as the interaction between each section. In addition to the GSHP system, an auxiliary system (conventional boiler or chiller) is also taken into consideration, if the GSHP system

Table 1
Material properties for the soil and pile domains.

Parameter	Sand	Concrete
Density [kg/m^3]	1990	2300
Poisson's Ratio []	0.3	0.2
Thermal Conductivity [W/(m·K)]	2.5	1.8
Specific Heat Capacity [J/(kg·K)]	1175	880

Table 2
Properties assigned for the pipe.

Property	Value
Inner Diameter [m]	0.0262
Pipe Wall Thickness [m]	0.0029
Thermal Conductivity [W/(m·K)]	0.41
Nominal Velocity of Flow [m/s]	3.7

is not competent in delivering the entire heating/cooling demand. The amount of energy supplied by the auxiliary system is particularly important in this study as it is essential to employ it in the LCA analysis.

The energy balance governing the building heating/cooling operation is shown below:

$$Q_{sec} = Q_{prim} + W_{hp} + Q_{aux} \tag{10}$$

where Q_{prim} is the energy supplied by the energy piles, W_{hp} is the energy input for the operation of the heat pump, and Q_{aux} is the energy to be supplied by an auxiliary system. The heating and cooling demands of the office building, which vary depending on the reference city and time, are introduced in the model (Fig. 1) to represent the secondary circuit (Q_{sec}).

The inlet ($T_{in,prim}$) and outlet ($T_{out, prim}$) temperatures of the water circulating within the piles are not constant but vary depending on the heating/cooling demand of the secondary circuit, coefficient of performance (COP) of the heat pump, as well as the heat transfer within the pipes and porous media.

The maximum COP of a heat pump is characterised by the source ($T_{out, prim}$) and delivery ($T_{in,sec}$) temperatures [30] in Kelvin (Fig. 3) while considering the reverse Carnot cycle for the heating (Eq. (10)) and cooling modes (Eq. (11)).

$$COP_{C,h} = \frac{T_{in,sec}}{T_{in,sec} - T_{out,prim}} \tag{11}$$

$$COP_{C,c} = \frac{T_{in,sec}}{T_{out,prim} - T_{in,sec}} \tag{12}$$

However, the Carnot COP represents the ideal reversible case, which cannot be achieved using a heat pump in practice. Therefore, the Carnot COP is multiplied by an efficiency factor to obtain the actual COP of the heat pump.

$$COP_{hp} = COP_C \eta_{hp} \tag{13}$$

where η_{hp} represents the efficiency factor and varies between 0.3 and 0.5 for small electric heat pumps and between 0.5 and 0.7 for efficient electric heat pumps [31]. Considering typical delivery temperatures for heating (45−90 °C for radiators) and cooling (5−15 °C for chilled water) operations, the possible COP values for a GSHP are presented in Fig. 4, wherein the delivery temperatures for heating and cooling are fixed at 65 °C and 5 °C, respectively.

As expected, the efficiency of the heat pump increases as the temperature difference between the source and delivery temperature decreases and as the efficiency factor increases. For the present study, a designated efficiency factor of 0.5 is used for the heat pumps in the three reference cities. An algorithm has been employed in the model, which determines the COP depending on the source temperature (Eqs. (10) and (11)); this allows the COP to vary with time for the reference cities.

In the presented model, the primary circuit of the system is completely modelled in the performed numerical analyses while the contributions provided by the GSHP, secondary circuit, and
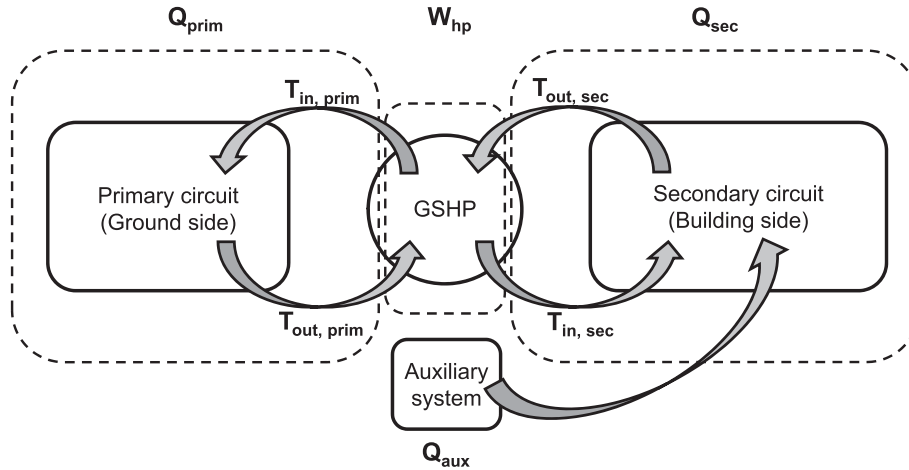
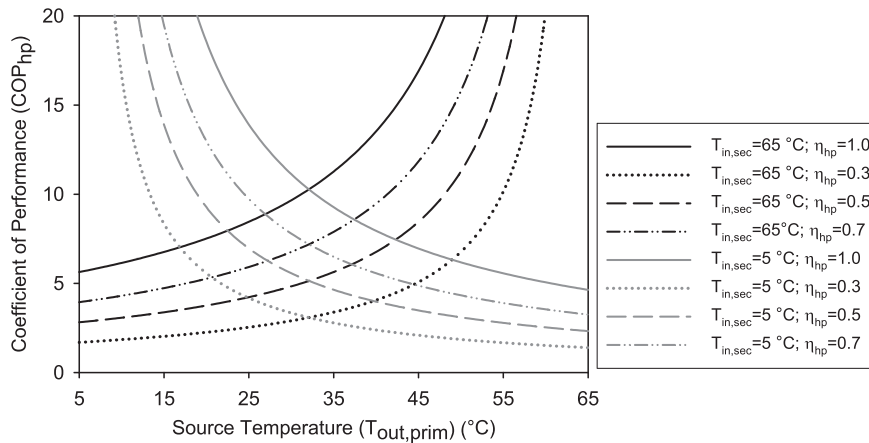**Fig. 3.** Scheme of a GSHP system.

Fig. 4. COP of GSHP with respect to the source temperature.

auxiliary system are idealised as described above. The idealised modelling of the GSHP and secondary circuit allows to achieve the fraction of the heating/cooling demand to be supplied by the energy piles (Q_{prim}), while the portion of the energy that cannot be supplied by the GSHP system is assumed to be covered by the auxiliary system.

2.2. Life cycle assessment

The environmental performance of energy piles should be compared with that of a conventional heating and cooling system to demonstrate its benefits from an environmental point of view. In this study, the LCA methodology is adopted to evaluate the potential environmental impacts while taking into consideration the material extraction, transportation, execution, use, and disposal. The analyses are performed by implementing the LCA model in the software SimaPro 8.0.3 [32].

The international standards ISO 14040, 2006 [33] and ISO14044 [34] describe the LCA methodology and the related analysis phases such as goal and scope definition, life cycle inventory (LCI), life cycle impact assessment (LCIA), and interpretation, which are followed in this study. The goal and scope definition step includes the definition of the functional unit (measure of the function of the system), the reference flow (quantitative reference unit required to satisfy the functional unit), and the boundaries of the system. In

this work, the functional unit has been defined as follows: "To fulfil the heating and cooling demands of an office building for one year". The considered design time spans of the building and the electric heating/cooling system were assumed to be 50 years and 20 years, respectively, and were accorded to the functional unit. The reference flow and system boundary are illustrated in Fig. 5. Two scenarios were selected in the present work to satisfy the annual heating and cooling demand for the three reference cities. In the first case, the function of the deep foundation was only to transfer the mechanical loads to the subsoil while a gas boiler and air conditioner were selected to meet the heating and cooling demands. In contrast, in the second case, the coupling between a group of energy piles and a GSHP was considered.

The flows between the investigated system and the environment, in terms of input and output products, resources, wastes, and emissions, were identified during the LCI. The input data of the LCI are reported in Tables 3 and 4 for the conventional system and energy piles, respectively. The amount of materials was obtained following the geotechnical design of the group of piles [35]. The transportation distance was hypothesised as 50 km while the drilling time was obtained in consultation with a specialised company. With respect to the use phase, the amount of energy required in terms of natural gas or electricity was obtained while considering the available heating and cooling demands and the results of the finite element analysis simulation reported in
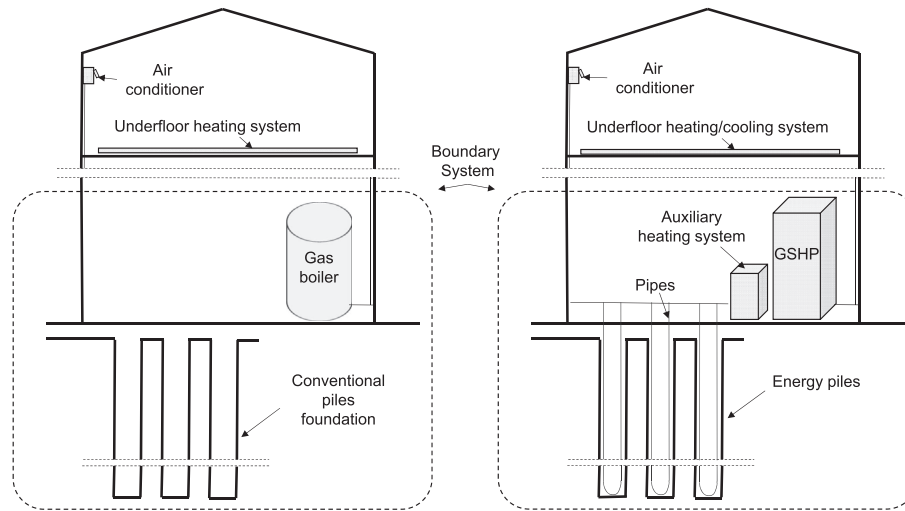
Fig. 5. a) Office building with pile foundation furnished by a conventional heating and cooling system; b) Office building equipped with energy piles.

Subsection 3.1. The latter allowed for the estimation of the geothermal energy that can be exploited by the thermal activation of the piles for the considered scenarios. According to the different heating and cooling demands and in situ temperature of the ground, the GSHP system behaves differently for each considered city, and therefore, the corresponding impact on the environment differs. With respect to the electricity supply, national flows were selected with respect to the three reference cities. The disposal scenario takes into consideration the recycling of all the involved materials, while assuming the recycling rates of the construction and demolition waste for the corresponding countries [36]. The last column of Tables 3 and 4 reports the selected environmental flow from the LCI database ecoinvent [37].

During the LCIA phase, the inventoried flows contributing to a given environmental impact category were achieved, the results of which are presented in terms of two main types of indicators selected at two different levels of the impact pathway: midpoint (Appendix) and end points (Section 3). The midpoint indicators usually indicate a change in the environment caused by a human intervention, while endpoint or damage indicators assess damages to (in the majority of cases) three areas of protection, i.e., human health, ecosystem quality, and resources. The Impact 2002+ [38] method was selected for performing the LCIA for all the considered cases. The end point results are presented in terms of climate change ($kgCO_{2,eq}$), human health (disability-adjusted life year–DALY), resource depletion (MJ), and ecosystem quality (potentially disappeared fraction of species $PDF \cdot m^2$/year).

The results of the LCA are presented for the three reference cities mentioned above in order to investigate the influence of the heating or cooling demands (direct consequences of the respective local climate) on the environmental performance of the investigated systems. Due to the difference in heating and cooling demands among the reference cities, the outputs of the FEM differ for each case which consequently affects the environmental analysis of the examined cases.

Table 3
LCI of the conventional systems for the three reference cities (SV: Seville; RM: Rome; BE: Berlin).

Life Cycle Step	Input	Amount SV/RM/BE	Unit	Flow from ecoinvent Database
Material Production	Concrete	6,51	m³	Concrete, normal {CH}
	Rebars	40,00	t	Reinforcing steel {GLO}
	Boiler	0,05/0,10/0.20	–	Oil boiler, 10 kW {CH}
Transportation	Concrete	795,00	tkm	Transport, freight, lorry 16–32 metric ton, EURO5 {GLO}
	Rebars	2,00	tkm	
	Machines	95,30	tkm	
	Transport of PipesTransport (EOL)	0,19	tkm	
		797,19	tkm	
Execution	Excavation	34,00	m³	Excavation, hydraulic digger {GLO}
	Drilling	1,00	hr	Machine operation, diesel, >=74.57 kW, high load factor {GLO}
Use	Heating	71,19/163,26/364,98	MWh	Heat, central or small-scale, natural gas {Europe without Switzerland}
	Cooling	142,44/138,93/20,88	MWh	Electricity, medium voltage {ES/IT/DE}
End of Life (EOL)	Boiler	12,20	kg	Used industrial electronic device {CH}
		0,15	kg	Inert waste, for final disposal {CH}
		3,35	kg	Waste reinforcement steel {CH}	collection for final disposal
		2,65	kg	Waste reinforcement steel {CH}| treatment of, recycling
		0,05	kg	Waste plastic, mixture {Europe without Switzerland}
		0,40	kg	Inert waste, for final disposal {CH}
	Reinforced concrete	15,93	t	Waste reinforced concrete {Europe without Switzerland}
		13,70	t	Waste concrete {Europe without Switzerland}
		−2,23	t	Recycling concrete (Rock crushing {RER}| processing
		5,60	t	Waste reinforcement steel {RoW}
	Soil	4,61	kg	Drilling waste {CH}| treatment of, residual material landfill

Table 4
LCI of energy piles for the three reference cities (SV: Seville; RM: Rome; BE: Berlin).

Life Cycle Step	Input	Amount SV/RM/BE	Unit	Flow from ecoinvent Database
Material Production	Concrete	6,50	m^3	Concrete, normal {CH}
	Rebars	40,00	kg	Reinforcing steel {GLO}
	GSHP	0,01/0,02/0.04	–	Heat pump, 30 kW {RER}
	Auxiliary System	0,00/0,26/0.66	-kg	Auxiliary heating unit, electric, 5 kW {CH}
	Refrigerant	3,94	kg	Refrigerant R134a {RER}
	Pipes	3,80	m	Extrusion, plastic pipes {RER}
		38,40		Polyethylene pipe, DN 200, SDR 41 {GLO}
Transportation	Concrete	795,00	tkm	Transport, freight, lorry 16–32 metric ton, EURO5 {GLO}
	Rebars	2,00	tkm	
	Machines	95,30	tkm	
	Transport of Pipes	0,19	tkm	
	Transport (EOL)	797,19	tkm	
Execution	Excavation	34,00	m^3	Excavation, hydraulic digger {GLO}
	Drilling	1,00	hr	Machine operation, diesel, >=74.57 kW, high load factor {GLO}
Use	Heating			
	Renewable	53,14/109,14/108,81	MWh	Energy, geothermal, converted
	Heat pump	19,26/56,08/104,39	MWh	Electricity, medium voltage {ES, IT, DE}
	Auxiliary	0,00/0,00/80,39	MWh	Electricity, medium voltage {ES, IT, DE}
	Cooling			
	Renewable	30,93/108,81/17,91	MWh	Energy, geothermal, converted
	Heat pump	5,31/24,97/3,79	MWh	Electricity, medium voltage {ES, IT, DE}
	Auxiliary	6,48/6,45/0,00	MWh	Electricity, medium voltage {ES, IT, DE}
End of Life (EOL)	GSHP	20,40	kg	Used industrial electronic device {CH}
		3,29	kg	Inert waste, for final disposal {CH}
		7,94	kg	Waste reinforcement steel {CH}| collection for final disposal
		6,26	kg	Waste reinforcement steel {CH}| treatment of, recycling
		0,29	kg	Waste plastic, mixture {Europe without Switzerland}
		0,15	kg	Inert waste, for final disposal {CH}
		1,00	kg	Used refrigerant R134a {GLO}|
	Reinforced concrete	15,90	t	Waste reinforced concrete {Europe without Switzerland}
		13,70	t	Waste concrete {Europe without Switzerland}
		−2,23	t	Recycling concrete (Rock crushing {RER}| processing
		5,60	kg	Waste reinforcement steel {RoW}
	Pipes	32,70	kg	polyethylene/polypropylene product {CH}
		0,53	kg	PE (waste treatment) {GLO}| recycling of PE
	Soil	4,61	t	Drilling waste {CH}| treatment of, residual material landfill

3. Results and discussion

Both the 3D finite element model (Section 2.1) and the LCA analysis (Section 2.2) were employed to reveal the long-term energy performance and environmental impacts of an energy pile project in three different cities (Seville, Rome, and Berlin).

Fig. 6 shows the influence of the intermittent operation of the GSHP on the water temperature circulating within the pipes during the transition from heating-to-cooling and cooling-to-heating operational modes. The example plot is given for Seville. The upper part of the figures shows the temperature of the water while the lower one shows the operation and stoppage periods within the same timeframe. The figure shows the decrease in the temperature of the circulating fluid with the operation of the heat pump during the heating mode, and the recovery (i.e., increase) of the temperature during the stoppage times, which is the contrary for the case of cooling. A temperature difference of 2–4 °C between the operation and stoppage times can be observed in the figure. The same simulation principle was applied for Rome and Berlin wherein the model was employed for 1 year without interruption.

In this section, the results of the analyses for the three cities under consideration are presented in terms of (i) energy demand and supply, (ii) temperature change along the energy piles and the surrounding soil, and (iii) LCIA in terms of climate change, human health, resources, and ecosystem quality.

3.1. Energy demand and supply

The comparison of the monthly heating and cooling demands from the building side and the available output from the primary circuit are presented in Fig. 7, along with the seasonal fluctuation of the heat carrier fluid. The demand/supply balance was checked iteratively at 30-min intervals for each day of the simulation, which resulted in a slightly higher supply as compared to the demand during some months if the demand was provided at a shorter time than 30 min. The comparison of the demand and supply shows that the majority of the heating and cooling demand in Seville was met by the GSHP, while an auxiliary cooling system was employed only for the month of July to cover the remaining 13% of the cooling demand (Fig. 7a). Similar results were obtained for Rome (Fig. 7b); although the heating demand was higher than that of Seville, the GSHP was capable of realising the required supply, while an auxiliary cooling system was required for the peak cooling periods (i.e., months of July for 11% and August for 6%). In the case of Berlin, the heating and cooling demands, which are characterised by dominant heating and limited cooling, were quite diverse as compared to the former two. The requirement of an auxiliary heating system for the four months of November (14%), December (33%), January (38%), and February (32%), i.e., during winter, can be observed in Fig. 7 c, while the limited cooling demand was met entirely by the GSHP.

The initial temperatures of the involved elements (i.e., soil, piles, pipes, and heat carrier fluid), which were considered to be constant, were determined by relating the air temperatures to the ground
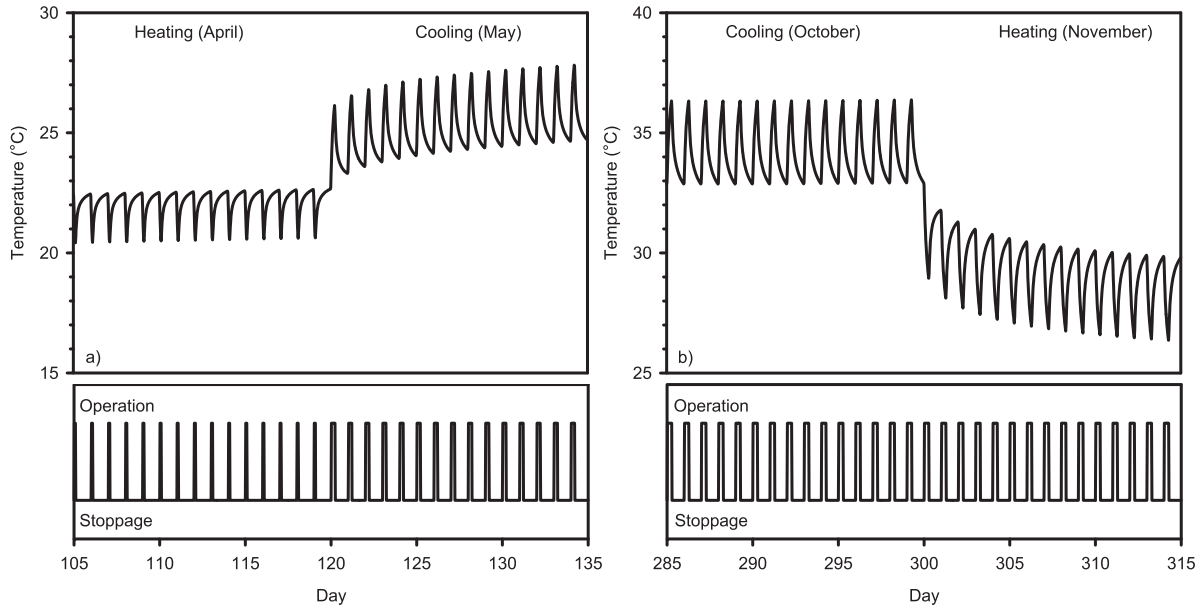
Fig. 6. Temperature fluctuation of the water circulating in the pipes due to intermittent operation of GSHP during transition from a) Heating to cooling, b) Cooling to heating (Seville).
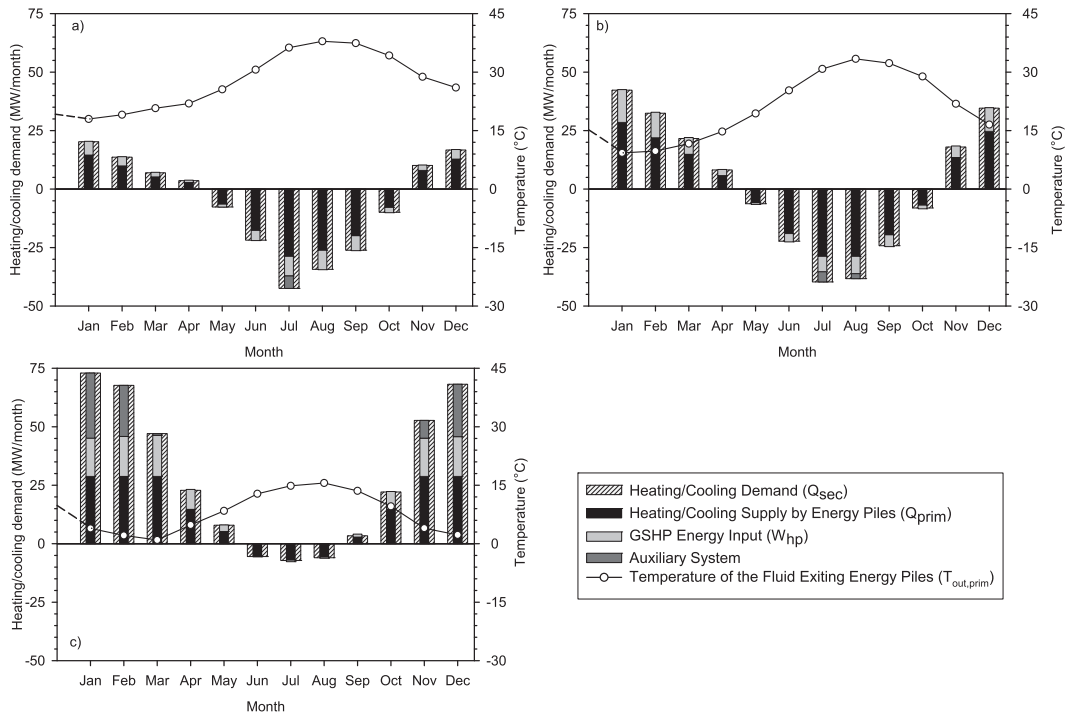

Fig. 7. Annual distribution of energy demand and supply; temperature of the heat carrier fluid for a) Seville, b) Rome, and c) Berlin cases.

temperatures, which corresponds to 19.2 °C, 15.2 °C, and 9.8 °C for Seville, Rome, and Berlin, respectively. The initial conditions also involved the temperature of the fluid exiting the energy piles ($T_{out, prim}$) as being originally equal to the average ground temperature. Following the start of the geothermal operations, $T_{out, prim}$ showed an annual fluctuation, which was associated with the corresponding heating and cooling demands from the building side. The temperature decrease during the heating operation which was followed by a recovery and a temperature increase period are in agreement with the case studies presented by Brandl [19].

3.2. Temperature fluctuations along energy piles and in the surrounding soil

As a result of their unique roles, the energy piles are exposed to daily and seasonal temperature variations during their lifetime. Temperatures in the pile and in the surrounding soil fluctuate during the day in between operation and stoppage times resulting in short-term temperature changes. Furthermore, there is a seasonal increase in temperatures after episodes of heat injection during summer followed by seasonal temperature reductions

during heat extraction in winter.

These temperature changes may cause axial displacements, additional axial stresses, and changes in the shaft resistance, with a daily and seasonal cyclic nature, along their lengths. Moreover, geothermal operations characterised by excessive heat extraction may cause temperatures along the energy piles to decrease below zero, eventually resulting in the formation of ice lenses in the adjacent soil. To prevent the freezing and thawing of the soil during successive heating and cooling operations, which are associated with heave and settlement, a minimum temperature of 2 °C on the shaft of the energy piles is recommended [19]. Finally, a change in the in situ temperature of the ground in the long-term due to geothermal operation of the energy piles should be prevented as it may have a significant impact on the efficiency of the GSHP system. Therefore, the appropriate prediction and monitoring of the temperature fluctuations along the energy piles and surrounding soil is of paramount importance.

To investigate this phenomenon, the temperature evolution along the centre pile and that in the surrounding soil during the geothermal operation in the three cities are presented in Fig. 8. The maximum temperature decrease and increase due to heat extraction and injection, respectively, and the residual temperature change along the energy pile after 1 year of geothermal operation are specified in the figure. The temperature variations with respect to the in situ temperature of the piles are within the typical range (±15–20 °C) for operating energy piles [39].

The comparison of the temperature variations along the energy pile and surrounding soil (Fig. 8) reveals that the soil closer to the energy pile (at a 1-m distance) exhibits a rapid response to the

geothermal operation with higher temperature variations, which lags behind and decreases in magnitude at a greater distance (2.4 m) from the piles. Moreover, the soil at a 2.4-m distance, which is equidistant from the two rows of energy piles, experiences temperature variations as well, although very limited, which evidences the thermal interactions between the neighbouring piles.

Considering the ground temperature variation during the geothermal operation of the energy piles, three types of thermal responses are observed in Fig. 8: (i) long-term temperature increase in the case of Seville due to cooling-dominant geothermal operation, (ii) thermal balance in the case of Rome, and (iii) long-term temperature decrease in the case of Berlin due to heating-dominant geothermal operation. Influences on the in situ temperature of the ground in the long-term should be avoided during geothermal operations, which significantly depends on the balance of the heating and cooling demands from the building side, as well as the ground water flow corresponding to the natural thermal recharge of the soil, which was not taken into consideration in the present study. In the case of low permeability, the balance between heat injection and extraction should be ensured for the long-term thermal equilibrium of the ground temperature. In contrast, in the case of soils characterised by high permeability, with a ground water flow greater than 0.5 m/day, the ground temperature equilibrium may be ensured by the groundwater flow, after unbalanced heating-cooling operations [40]. Therefore, a special thermal design for the specific GSHP operations is of paramount importance for taking into consideration the space heating/cooling needs and hydrogeological ground conditions, in order to ensure that despite seasonal fluctuations, the in situ ground temperature remains the same in the long-term.
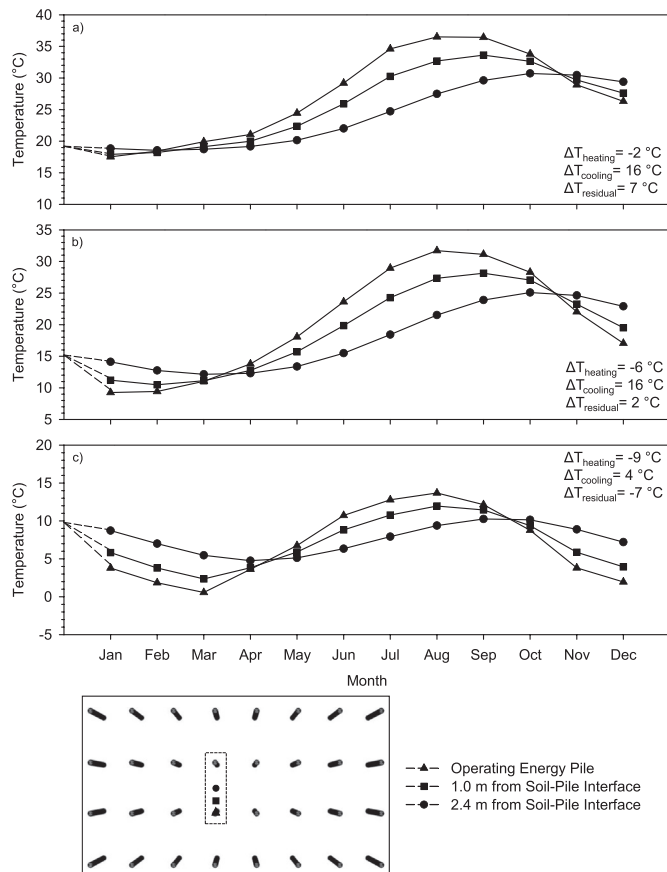
3.3. Life cycle impact assessment

The results reported in Section 3.1 in combination with the available data from the ENTRANZE Project were used for the LCI of the two systems (i.e., conventional piles and energy piles) for the three reference scenarios (Section 2.2).

The first remarkable outcome of the LCIA is the confirmation that the heating and cooling (use phase) are the main contributors to the climate change impact with respect to the other life cycle stages (material production, transportation, execution, and end of
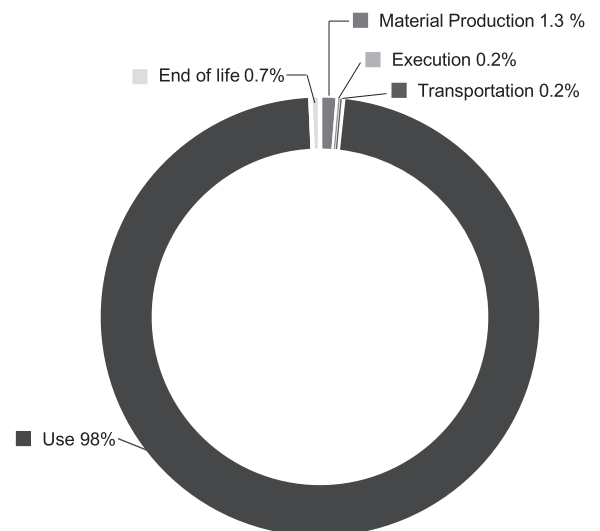

Fig. 8. Pile and soil temperature during geothermal operations in a) Seville, b) Rome, and c) Berlin.

Fig. 9. Contribution to the total environmental impact in terms of climate change from the different LC stages (average of the three reference cities).

life). Considering a conventional pile foundation and a conventional heating and cooling system, Fig. 9 shows that the use phase contributes up to 98% of the total climate change impact while the residual 2% is represented by the other steps of the geostructure LC (e.g., material production, transportation, execution, and end of life). These results clearly identify the LC phase wherein it is potentially possible to reduce the impact on the environment. The energy piles, exploiting the geothermal energy in principle and can

aid in reducing the impacts of the use phase. Nevertheless, there are a number of key points that are required to be considered before arriving at this conclusion: additional materials (i.e., pipes, GSHP, and auxiliary system) and different energy sources are required to be introduced in the LC of the system while adopting the energy piles concept. Moreover, the environmental performance is highly dependent on the heating and cooling demands (i.e., the local climate), which consequently varies during the different periods of
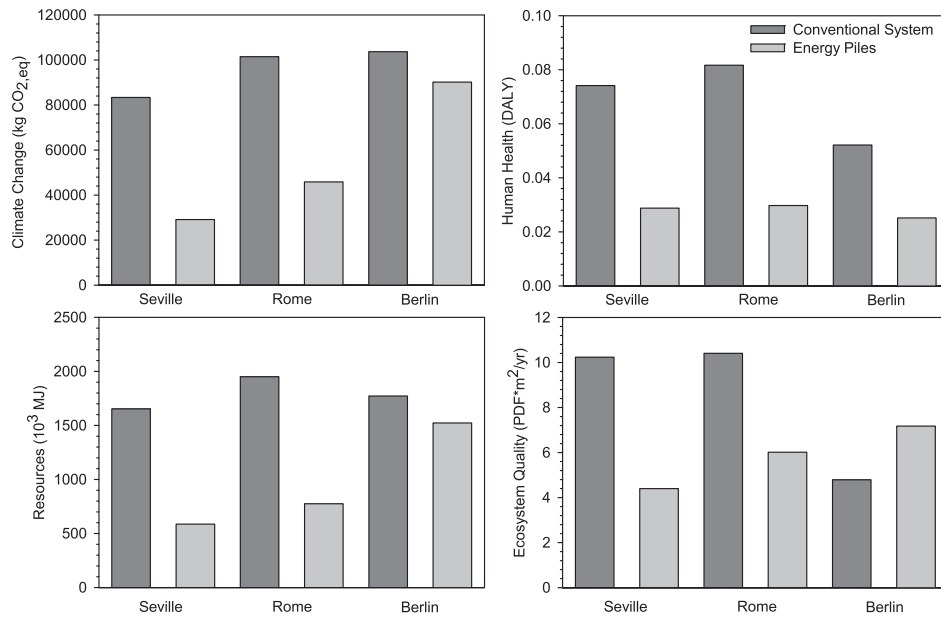

Fig. 10. Indicators of the environmental performance of the conventional system and the energy piles for the three reference cities.
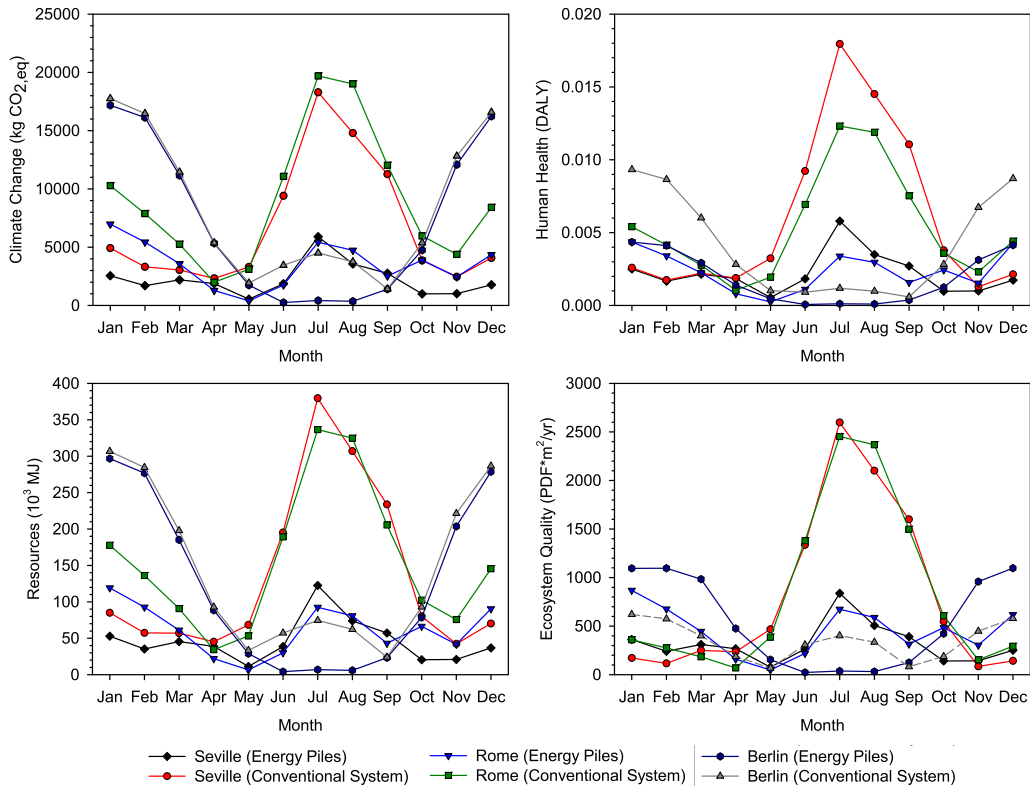

Fig. 11. Evolution of the environmental indicators of the conventional system and the energy piles during the reference year for the three reference cities.

the year. Finally, the way the energy is produced to satisfy heating and cooling needs differs depending on the country under consideration. Therefore, despite introducing the same energy source in an LC model, it can result in different environmental impacts as the country under consideration changes. The outcomes of the LCIA are used in this study to examine these features.

Fig. 10 shows the results of the LCIA in terms of the four "endpoint" indicators employed by the Impact2002 + method, while the "midpoint" indicators are reported in the appendix, in Figs. A.1, A.2, and A.3. It is directly noticeable that the environmental performance of both investigated systems strongly depends on the countries and the heating and cooling demands. For example, on only considering the conventional system, the indicators presented different scores for the three reference cities (e.g., for climate change: Seville 83358 $kgCO_{2eq}$, Rome 101457 $kgCO_{2eq}$, and Berlin 103700 $kgCO_{2eq}$). Generally, the environmental analysis rewarded the energy piles that showed a considerable reduction of impacts.

With reference to the cities of Seville and Rome, the score of all the indicators was significantly in favour of the energy piles, which showed a reduction of 65% and 55% in terms of the equivalent CO_2 emissions, 61% and 64% in terms of human health, 64% and 60% in terms of resources depletion, and 57% and 42% in terms of ecosystem quality, respectively.

A lower reduction of the impacts was found in the case of Berlin: 13% in terms of climate change, 52% for human health, and 14% for resources depletion. The ecosystem quality was the only score in favour of the conventional system. Based on the midpoint indicators reported in the appendix, the ecosystem-related midpoint indicators in line with endpoint results for ecosystem quality are ionising radiation, land occupation, ozone layer depletion, terrestrial ecotoxicity, and mineral extraction. These results are explained by the high amount of auxiliary energy required to meet the heating demand in Berlin, which was not satisfied by exploiting only the geothermal source, and the consequential high electricity demand for the use of the energy pile system.

Moreover, the analysis of the midpoints reported in the appendix clearly illustrates why energy piles have a negative impact on the ozone layer depletion in each city. This is due to the presence of refrigerant in the infrastructure of the heat pump.

Fig. 11 reports a detailed overview of the environmental indicators for all the considered scenarios. The results are reported for each month of the reference year. As was expected, the peak values of the indicators can be identified during winter for the case of Berlin and during summer for Seville and Rome. It is interesting to note that, on comparing the conventional system with the energy piles during the reference year, a reduction in the impacts during the heating periods was always noted, but during the cooling periods, the energy piles contributed significantly to reducing the score of the indicators. This means that the energy piles not only contributed to providing a clean energy source for the heating of the building but they were especially efficient from an environmental point of view during the cooling periods. This is a significant advantage for the energy piles over other technologies exploiting renewable energy, which mainly satisfy only the heating demand.

4. Conclusions

This paper presents the long-term performance of a group of energy piles in terms of meeting the heating and cooling demands of a reference office building in three different climatic conditions. For this purpose, a 3D finite element model was developed, which is capable of taking into consideration the intermittent operation of a GSHP, as well as the heating and cooling demands from the building side with a monthly varying nature. The results obtained on using the finite element model, in terms of meeting the heating

and cooling demands from the building side, were employed to perform an LCA analysis.

With this study, finally a quantitative comparison of the environmental impact between a conventional heating and cooling system and energy piles has been presented in terms of climate change, resource consumption, human health, ecosystem quality. The comparison among three reference climate scenarios has provided clear evidences regarding the adoption of the energy pile system in the selected areas. With the use of energy piles, the LCA demonstrated a reduction in terms of equivalent CO_2 emissions, human health, resources depletion, and ecosystem quality for Seville and Rome, respectively, while the reduction was lower in the case of Berlin. The comparison of the conventional and GSHP systems showed that the energy piles yielded the highest reduction in indicators during the cooling periods, which is considered to be partially related to the higher coefficient of performance of the GSHP during summer months. According to this study, the energy pile technology, providing a clean energy source for both heating and cooling of the buildings, is more efficient from an environmental point of view compared to conventional systems. Moreover, their environmental performance has revealed to be especially satisfactory during the cooling periods, which is a significant advantage with respect to other renewable energy technologies satisfying solely the heating demand.

Declarations of interest

None.

Nomenclature

Symbol	Name	Unit
Roman Symbols		
A_p	Cross sectional area of pipe	m^2
c	Specific heat capacity	$J/(kg \cdot K)$
c_f	Specific heat capacity of the fluid	$J/(kg \cdot K)$
COP	Coefficient of performance of the heat pump	−
$COP_{C,c}$	Carnot coefficient of performance for cooling	−
$COP_{C,h}$	Carnot coefficient of performance for heating	−
d_h	Hydraulic diameter of the pipe	m
f_D	Darcy friction factor	−
h_{eff}	Effective heat transfer coefficient of the pipe	$W/(m^2 \cdot K)$
h_{int}	Convective heat transfer coefficient inside the pipe	$W/(m^2 \cdot K)$
Nu	Nusselt number	−
Nu_{turb}	Nusselt number under turbulent flow conditions	−
Pr	Prandtl number	−
q'_w	Heat transfer through the unit length of the pipe wall	W/m
Q_{aux}	Energy supplied by the auxiliary system	W
Q_{prim}	Energy supplied by the energy piles	W
Q_{sec}	Energy supplied to the building	W
Re	Reynolds number	−
r_{in}	Inner diameter of the pipe	m
r_{out}	Outer diameter of the pipe	m
T	Temperature	K
T_f	Temperature of the fluid	K
T_{out}	Outer temperature of the pipe	K
t	Time	s
$u_{f,i}$	Fluid velocity vector	m/s
Greek Symbols		
λ	Thermal conductivity	$W/(m \cdot K)$
λ_f	Thermal conductivity of the fluid	$W/(m \cdot K)$
λ_p	Thermal conductivity of the pipe	$W/(m \cdot K)$
η_{hp}	Efficiency factor of the heat pump	−
ρ	Density	kg/m^3
ρ_f	Density of the fluid	kg/m^3

Acknowledgements
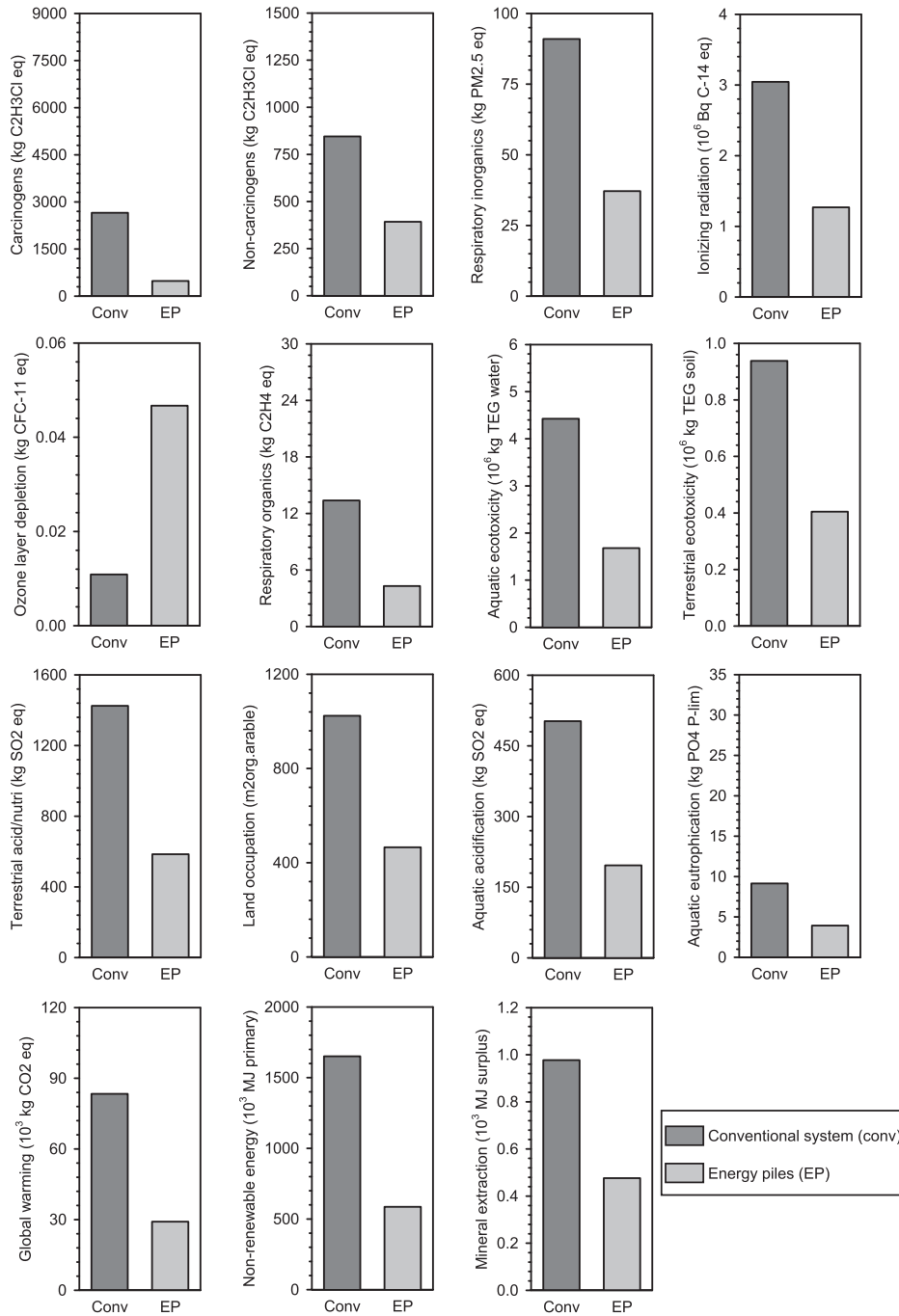
Appendix. A

Fig. A.1. Midpoint indicators of the conventional system and the energy piles for Seville.
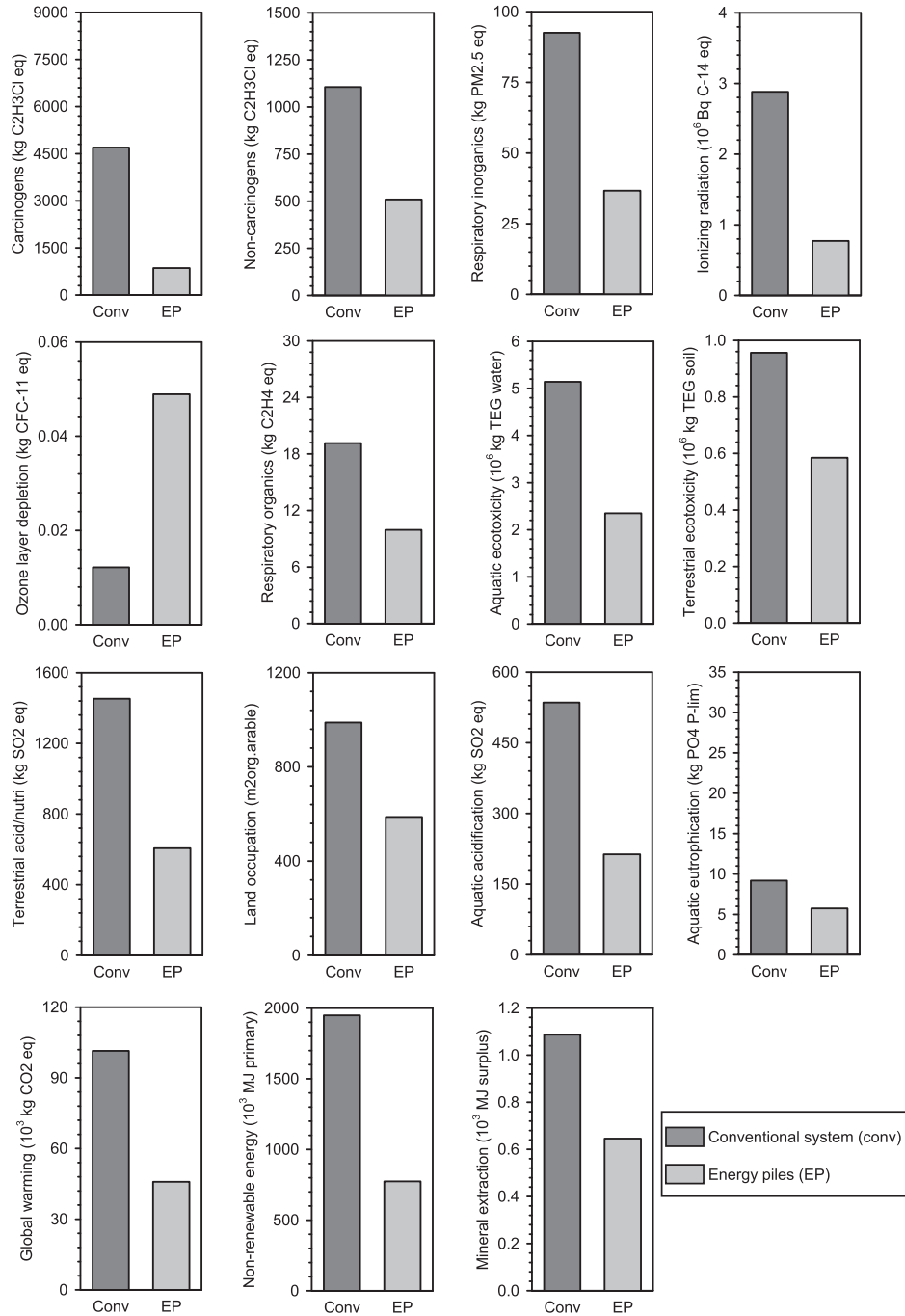
Fig. A.2. Midpoint indicators of the conventional system and the energy piles for Rome.
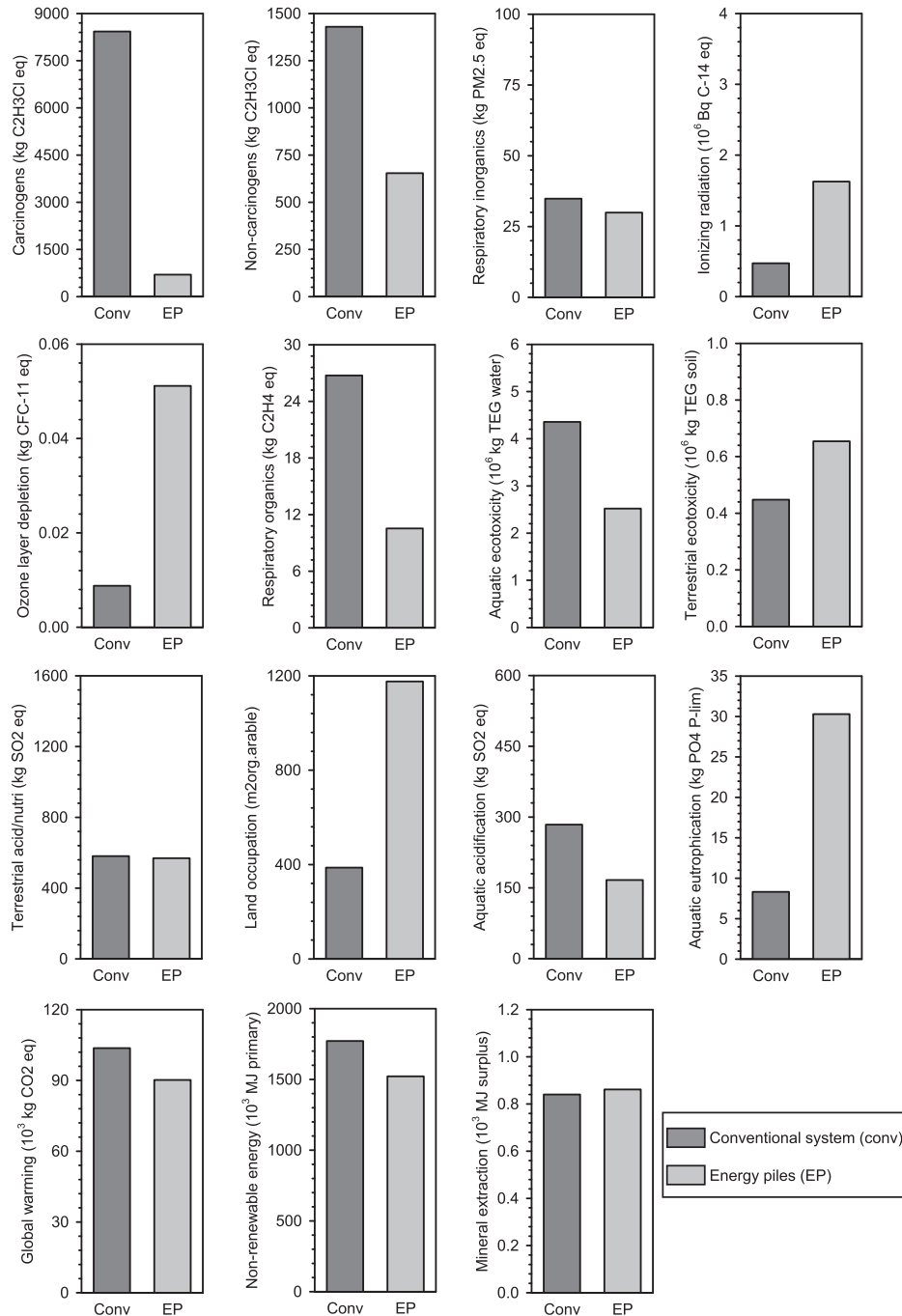
Fig. A.3. Midpoint indicators of the conventional system and the energy piles for Berlin.

References

[1] International Energy Agency, I. E. A, World Energy Outlook 2017, OECD Publishing, Paris/IEA, Paris, 2017. https://doi.org/10.1787/weo-2017-en.

[2] European Commission, An EU Strategy on Heating and Cooling, COM, European Commission, Brussels, Belgium, 2016, p. 51 Final, 2016.

[3] International Energy Agency, I. E. A, last updated, https://www.iea.org/tcep/buildings/, 2019. (Accessed 25 January 2019).

[4] International Energy Agency, I. E. A, last updated, https://www.iea.org/tcep/buildings/heating/, 2019. (Accessed 13 March 2019).

[5] International Energy Agency, I. E. A, The Future of Cooling, OECD Publishing, Paris/IEA, Paris, 2018.

[6] L. Laloui, M. Nuth, L. Vulliet, Experimental and numerical investigations of the behaviour of a heat exchanger pile, Int. J. Numer. Anal. Methods Geomech. 30 (8) (2006) 763–781. https://doi.org/10.1002/nag.499.

[7] P.J. Bourne-Webb, B. Amatya, K. Soga, T. Amis, C. Davidson, P. Payne, Energy pile test at Lambeth College, London: geotechnical and thermodynamic aspects of pile response to heat cycles, Geotechnique 59 (3) (2009) 237–248, https://doi.org/10.1680/geot.2009.59.3.237.

[8] S. You, X. Cheng, H. Guo, Z. Yao, Experimental study on structural response of CFG energy piles, Appl. Therm. Eng. 96 (2016) 640–651. https://doi.org/10.1016/j.applthermaleng.2015.11.127.

[9] T. Mimouni, L. Laloui, Behaviour of a group of energy piles, Can. Geotech. J. 52 (12) (2015), https://doi.org/10.1139/cgj-2014-0403, 1913–192.

[10] M. Faizal, A. Bouazza, R.M. Singh, An experimental investigation of the influence of intermittent and continuous operating modes on the thermal behaviour of a full scale geothermal energy pile, GeoMech. Energy Environ. 8 (2016) 8–29. https://doi.org/10.1016/j.gete.2016.08.001.

[11] A.F. Rotta Loria, L. Laloui, Thermally induced group effects among energy piles,

Geotechnique 67 (5) (2016) 374–393. https://doi.org/10.1680/jgeot.16.P.039.

[12] M. Sutman, T. Brettmann, C.G. Olgun, Full-scale in-situ tests on energy piles: head and base-restraining effects on the structural behaviour of three energy piles, GeoMech. Energy Environ. 18 (2019) 56–68. https://doi.org/10.1016/j.gete.2018.08.002.

[13] C. Knellwolf, H. Peron, L. Laloui, Geotechnical analysis of heat exchanger piles, J. Geotech. Geoenviron. Eng. 137 (10) (2011) 890–902, https://doi.org/10.1061/(ASCE)GT.1943-5606.0000513.

[14] P. Bourne-Webb, J.M. Pereira, G.A. Bowers, T. Mimouni, F.A. Loveridge, S. Burlon, C.G. Olgun, J.S. McCartney, M. Sutman, Design tools for thermoactive geotechnical systems, DFI J. J. Deep Found. Inst. 8 (2) (2014) 121–129. https://doi.org/10.1179/1937525514Y.0000000013.

[15] D. Salciarini, F. Ronchi, E. Cattoni, C. Tamagnini, Thermomechanical effects induced by energy piles operation in a small piled raft, Int. J. Geomech. 15 (2) (2013), 04014042, https://doi.org/10.1061/(ASCE) GM.1943-5622.0000375.

[16] A.F. Rotta Loria, L. Laloui, The interaction factor method for energy pile groups, Comput. Geotech. 80 (2016) 121–137. https://doi.org/10.1016/j.compgeo.2016.07.002.

[17] N. Makasis, G.A. Narsilio, A. Bidarmaghz, A machine learning approach to energy pile design, Comput. Geotech. 97 (2018) 189–203. https://doi.org/10.1016/j.compgeo.2018.01.011.

[18] M. Sutman, C.G. Olgun, L. Laloui, Cyclic load–transfer approach for the analysis of energy piles, J. Geotech. Geoenviron. Eng. 145 (1) (2018), 04018101, https://doi.org/10.1061/(ASCE)GT.1943-5606.0001992.

[19] H. Brandl, Energy foundations and other thermo-active ground structures, Geotechnique 56 (2) (2006) 81–122. ISSN 0016-8505.

[20] F.A. Loveridge, W. Powrie, T. Amis, M. Wischy, J. Kiauk, Long term monitoring of CFA energy pile schemes in the UK, Energy Geotechnics, 2016, pp. 585–592. https://doi.org/10.1201/b21938-92.

[21] J.S. McCartney, K.D. Murphy, Investigation of potential dragdown/uplift effects on energy piles, GeoMech. Energy Environ. 10 (2017) 21–28. https://doi.org/10.1016/j.gete.2017.03.001.

[22] D. Basu, A. Misra, A.J. Puppala, Sustainability and geotechnical engineering: perspectives and review, Can. Geotech. J. 52 (1) (2014) 96–113. https://doi.org/10.1139/cgj-2013-0120.

[23] Entranze Policies to Enforce the Transition to Nearly Zero Energy Buildings in the EU-27, accessed June 2019, https://www.entranze.eu/.

[24] P. Zangheri, R. Armani, M. Pietrobon, L. Pagliano, M.F. Boneta, A. Müller, Heating and Cooling Energy Demand and Loads for Building Types in Different Countries of the EU, Polytechnic University of Turin, end-use Efficiency Research Group, 2014, p. 3.

[25] COMSOL Multiphysics® v. 5.3, COMSOL AB, Stockholm, Sweden, www.comsol.com.

[26] S.E. Haaland, Simple and explicit formulas for the friction factor in turbulent pipe flow, J. Fluids Eng. 105 (1) (1983) 89–90, https://doi.org/10.1115/1.3240948.

[27] C.F. Colebrook, Turbulent flow in pipes with particular reference to the transition region between the smooth and rough pipe laws, J. Inst. Civ. Eng. 12 (8) (1939) 393–422. https://doi.org/10.1680/ijoti.1939.14509.

[28] T. Kusuda, P.R. Achenbach, Earth Temperature and Thermal Diffusivity at Selected Stations in the United States (No. NBS-8972), National Bureau of Standards, Gaithersburg MD, 1965.

[29] V. Ionescu, A.A. Neagu, Finite element method analysis of a MEMS-based heat exchanger with different channel geometries, Energy Procedia 112 (2017) 158–165, https://doi.org/10.1016/j.egypro.2017.03.1077.

[30] I. Sarbu, C. Sebarchievici, General review of ground-source heat pump systems for heating and cooling of buildings, Energy Build. 70 (2014) 441–454. https://doi.org/10.1016/j.enbuild.2013.11.068.

[31] S. Kärkkäinen, E. Oy, Heat Pumps for Cooling and Heating. International Energy Agency Demand-Side Management Programme Task VXII, 2012. IEADSM report.

[32] PRe Consultants. SimaPro (8.0.3.), LCA Software. Amersfoort, the Netherlands, 2014 (accessed May 2019), https://simapro.com/.

[33] ISO, ISO 14040, Environmental Management - Life Cycle Assessment - Principle and Framework, 2014.

[34] ISO, ISO 14044, Environmental Management – Life Cycle Assessment – Requirements and Guidelines, 2006.

[35] EN 1997, Eurocode 7: Geotechnical Design. London, United Kingdom, 2004, p. 171.

[36] V. Monier, M. Hestin, M. Trarieux, S. Mimid, L. Domrose, M. Van Acoleyen, S. Mudgal, Service Contract on Management of Construction and Demolition Waste, Report EU Commission, 2013.

[37] G. Wernet, C. Bauer, B. Steubing, J. Reinhard, E. Moreno-Ruiz, B. Weidema, The ecoinvent database version 3 (part I): overview and methodology, Int. J. Life Cycle Assess. 21 (9) (2016) 1218–1230, https://doi.org/10.1007/s11367-016-1087-8.

[38] O. Jolliet, M. Margni, R. Charles, S. Humbert, J. Payet, G. Rebitzer, R. Rosenbaum, IMPACT 2002+: a new life cycle impact assessment methodology, Int. J. Life Cycle Assess. 8 (6) (2003) 324, https://doi.org/10.1007/BF02978505.

[39] GSHP Association, Thermal Pile Design, Installation and Materials Standards, Ground Source Heat Pump Association, National Energy Centre, Davy Avenue, Knowlhill, Milton Keynes, MK5 8NG, 2012.

[40] L. Laloui, A. Di Donna, Understanding the behaviour of energy geo-structures, Proc. Inst. Civ. Eng. 164 (4) (2011) 184. https://search.proquest.com/docview/904929157?accountid=27198.